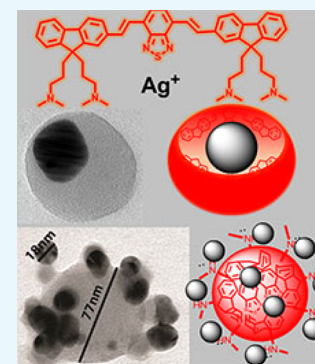


# One-Pot Synthesis of Hybrid Conjugated Oligomer-Ag Nanoparticles

Timuçin Balkan,<sup>†,‡</sup> Seda Kizir,<sup>†</sup> and Dönüş Tuncel<sup>\*,†,‡</sup>

<sup>†</sup>Department of Chemistry and <sup>‡</sup>UNAM–National Nanotechnology Research Center, Institute of Materials Science and Nanotechnology, Bilkent University, 06800 Ankara, Turkey

**ABSTRACT:** Here we report one-pot, straightforward synthesis of hybrid conjugated oligomer-silver nanoparticles (AgNPs) by utilizing tertiary alkyl amine and fluorene-benzothiazole-containing conjugated oligomer that both acts as a reducing agent in the reduction of silver ions into metallic silver and as a matrix to accommodate the newly formed AgNPs. By tuning the reaction conditions, it is possible to control the sizes and the structural features of hybrid nanoparticles as either raspberry or core-shell type hybrid structures.



## INTRODUCTION

Hybrid organic–inorganic nanostructures containing metals (e.g., Ag and Au) and polymers are very intriguing materials, as they combine the flexible and tailorable features of polymers with optical, electrical, and photophysical properties of metals, and because of these synergistic properties, they can find applications in areas including catalysis, plasmonic lasers, sensing, and theranostics.<sup>1–6</sup>

Hybrid nanoparticles of polymers with Au or Ag can be prepared by chemical reduction of Au or Ag salts using a variety of polymers.<sup>7–18</sup> Sodium borohydride (NaBH<sub>4</sub>) is one of most widely used reducing agents, but recently, the need of additional reducing agents like NaBH<sub>4</sub> has been eliminated by employing polymers as both reducing and stabilizing agents.<sup>7–17</sup> Hybrid NPs can be prepared in organic solvents or in aqueous media depending on the polymers used. For the preparation of water-dispersible hybrid nanoparticles, usually amphiphilic block copolymers<sup>10–15</sup> that can self-assemble into micellar or vesicle structures in water or water-soluble hyperbranched polymers<sup>8</sup> and dendrimers<sup>17</sup> are used because the interior of these nanostructures can accommodate metal ions in high concentration and act as a microreactor to facilitate the reduction of metal ions without the need of extra reducing agents and subsequently stabilize the newly formed metal nanoparticles.

As can be seen from the above literature examples, there are numerous studies on functionalizing of Au or Ag NPs with polymers, but the examples are relatively scarce on the use of conjugated and light-emitting polymers or oligomers for functionalization of Au or Ag NPs, although the synergistic effect of the both materials could offer many opportunities in the areas of nanophotonics and theranostics. For instance, gold and silver nanostructured materials having surface plasmon resonance (SPR) in the near-infrared region (NIR) have been widely used for NIR-mediated photothermal therapy (PTT). It

would also be possible to combine photothermal (PTT) and photodynamic therapies in a single theranostic platform.<sup>19</sup> For this purpose, organic dye-based photosensitizers that exhibit the photodynamic effect upon light irradiation have been incorporated to the gold or silver nanoparticles.<sup>20</sup> However, these dyes are usually attached to metal nanoparticles through noncovalent interactions that might cause the leakage of these dyes and a decrease in the efficiency. Moreover, these small organic dyes suffer from low photostability.

To this end, the hybrid of Ag or Au with conjugated polymer nanoparticles (CPNs) could be a good candidate for this and for many other applications because of CPNs' easy synthesis, tailorable chemical structures with desired functionalities, intrinsic and tunable emission properties, negligible toxicities, and high photostabilities.<sup>21–23</sup> Owing to these features they have been used in a variety of applications spanning from photonics to biomedical areas.<sup>21–33</sup> In the literature there are also some examples for hybrid nanostructures of CPNs with metal nanoparticles.<sup>34,35</sup> In these examples, usually prepared gold nanoparticles were mixed with conjugated polymers to form raspberry-type hybrid particles or embedded into conjugated polymer nanoparticles.<sup>36–42</sup> The photocatalytic applications of these nanoparticles have also been demonstrated.<sup>43,44</sup>

However, in the literature, to the best of our knowledge, there are no examples on the one-pot synthesis of hybrid nanoparticles of conjugated oligomers/polymers and silver/gold nanoparticles, in which the oligomer or polymer acts as a reducing agent to reduce the metal ions to form nanoparticles as well as acts as a matrix to hold the newly formed metal nanoparticles.

**Received:** June 27, 2017

**Accepted:** August 23, 2017

**Published:** September 6, 2017

Scheme 1. Schematic Presentation of the Synthesis of Hybrid COL-Ag NPs Using Two Different Approaches

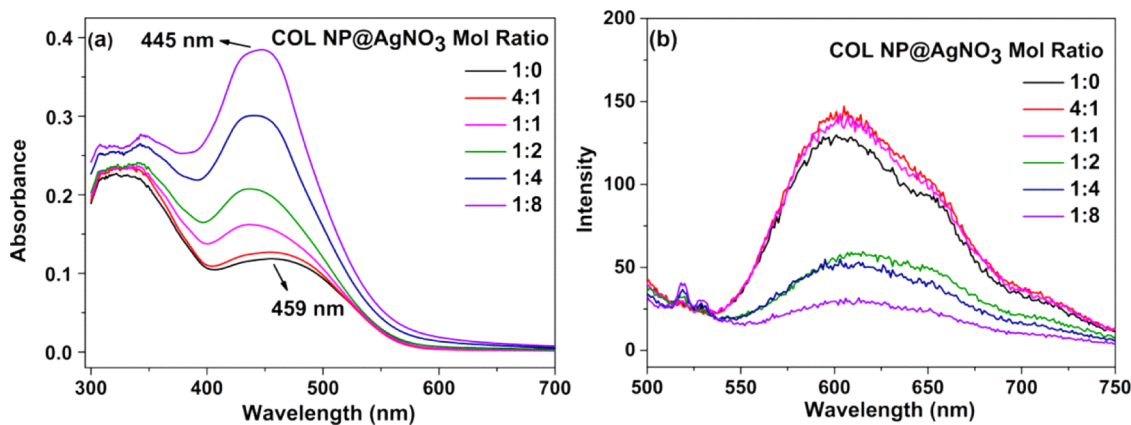
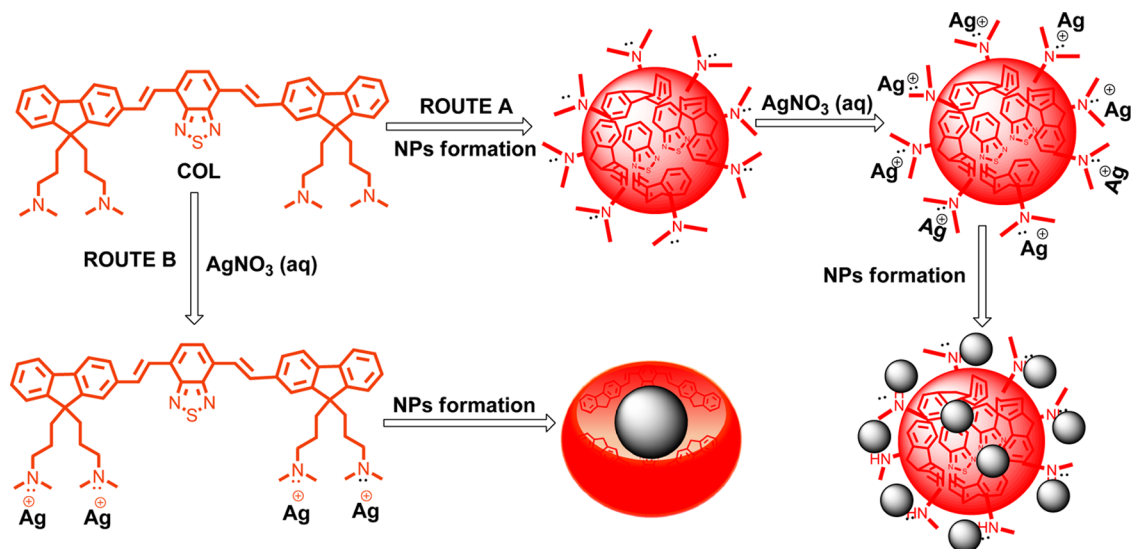


**Figure 1.** (a) UV-vis absorption and (b) PL spectra of COL-NP only and COL-NP@AgNP at 25 °C, with increasing concentration of Ag.

In this context, here, we report the one-pot, straightforward synthesis of hybrid conjugated oligomer/Ag nanoparticles. Tertiary alkyl amine and fluorene-benzothiadiazole-containing conjugated oligomer acted as reducing agents for reducing Ag ions into Ag(0) and then as a matrix to encapsulate and provide binding sites for the newly formed silver nanoparticles (AgNPs). Using this conjugated oligomer, it is possible to tune the structural features of hybrid nanoparticles. Hybrid NPs can be prepared in the form of raspberry-type structures, in which AgNPs will form in situ on the periphery of preprepared conjugated oligomer nanoparticles (COL-NPs) or core-shell type structures. We have also preliminarily shown that this approach could be applied for the reduction of gold ions to prepare hybrid gold nanoparticles.

## RESULTS AND DISCUSSION

**Synthesis.** In this work, red-emitting conjugated oligomer (COL), namely, 3,3',3'',3'''-[[[(1E,1'E)-2,1,3-benzothiadiazole-4,7-diylbis(ethene-2,1-diyl)]-bis(9H-fluorene-9,9,2-triyl)]-tetrakis(*N,N*-dimethylpropan-1-amine)], and its nanoparticle dispersion in water, for which the synthesis and characterization were reported in our previous publications, was used.<sup>30,33</sup>

To prepare hybrid nanoparticles of conjugated oligomer and silver, we have adopted two different routes, as shown in

**Scheme 1.** In the first route (route A), we have first prepared COL-NP using the nanoprecipitation method, in which COL was dissolved in tetrahydrofuran (THF) and the THF solution of COL was injected into large excess of water under sonication. THF was evaporated off to obtain aqueous dispersion of COL nanoparticles (COL-NP). To this aqueous dispersion of COL-NPs, aqueous solution of silver nitrate was added in varying ratios. The reaction was followed by UV-vis absorption spectroscopy over time.

In the second route (route B), instead of first preparing the oligomer nanoparticles and then adding the aqueous solution of AgNO<sub>3</sub> to allow AgNP formation, we have injected COL THF solution into aqueous AgNO<sub>3</sub> solution at predetermined ratios while rapidly stirring. In this way, COL chains self-assembled to form hybrid NPs by encapsulating the silver ions when they were exposed to water and Ag ions. Again, the reaction was monitored by UV-vis absorption spectroscopy by following the appearance of the plasmonic band of AgNP at around 430 nm.

**Details of Route A.** COL-NPs were prepared briefly, as follows. COL solution in THF (1 mg/mL) was injected into water under sonication, and the sonication has continued for about 30 min. THF was removed under reduced pressure to obtain water-dispersible red-emitting COL-NPs. The hydrodynamic diameter of the COL-NPs was determined by dynamic

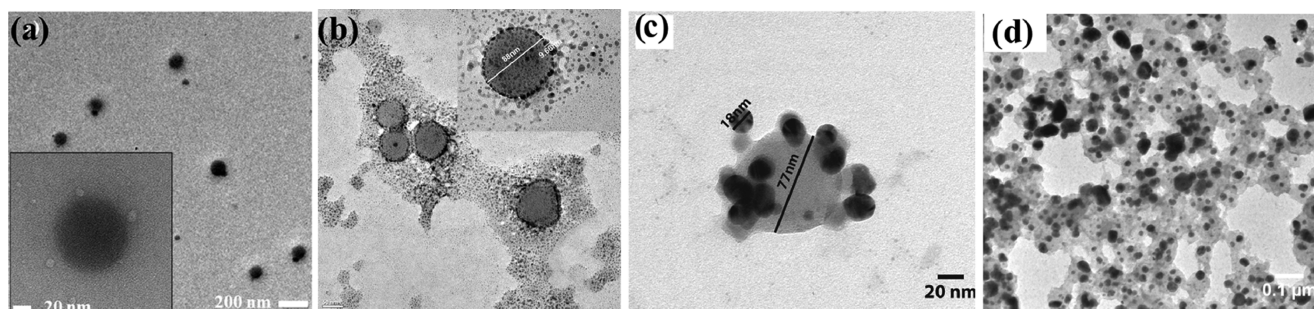


**Figure 2.** TEM images of (a) COL-NP only; (b) COL-NP@AgNO<sub>3</sub>, 24 h later; (c) COL-NP@AgNO<sub>3</sub>, 48 h later; and (d) COL-NP@AgNO<sub>3</sub>, 1 week later.

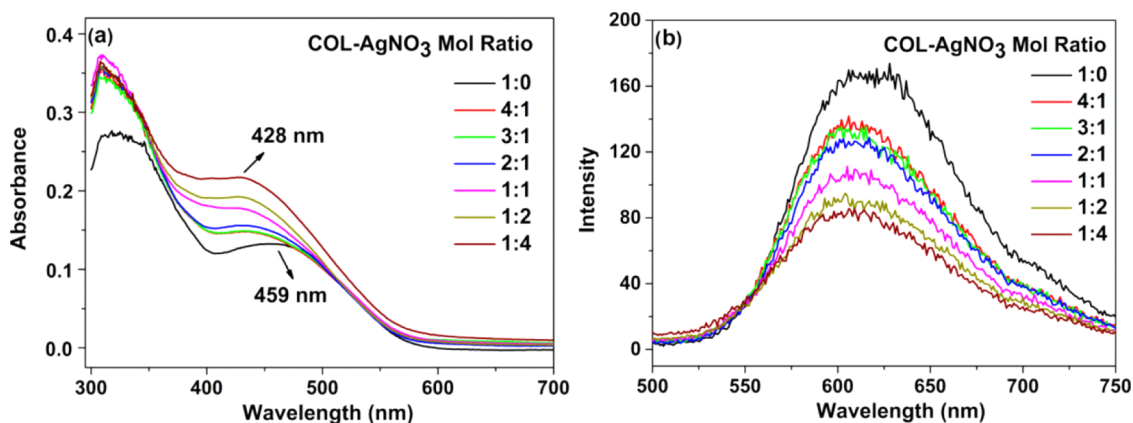


**Figure 3.** (a) UV-vis absorption and (b) PL spectra of hybrid COL-Ag NPs prepared at varying ratios of COL to AgNO<sub>3</sub>.

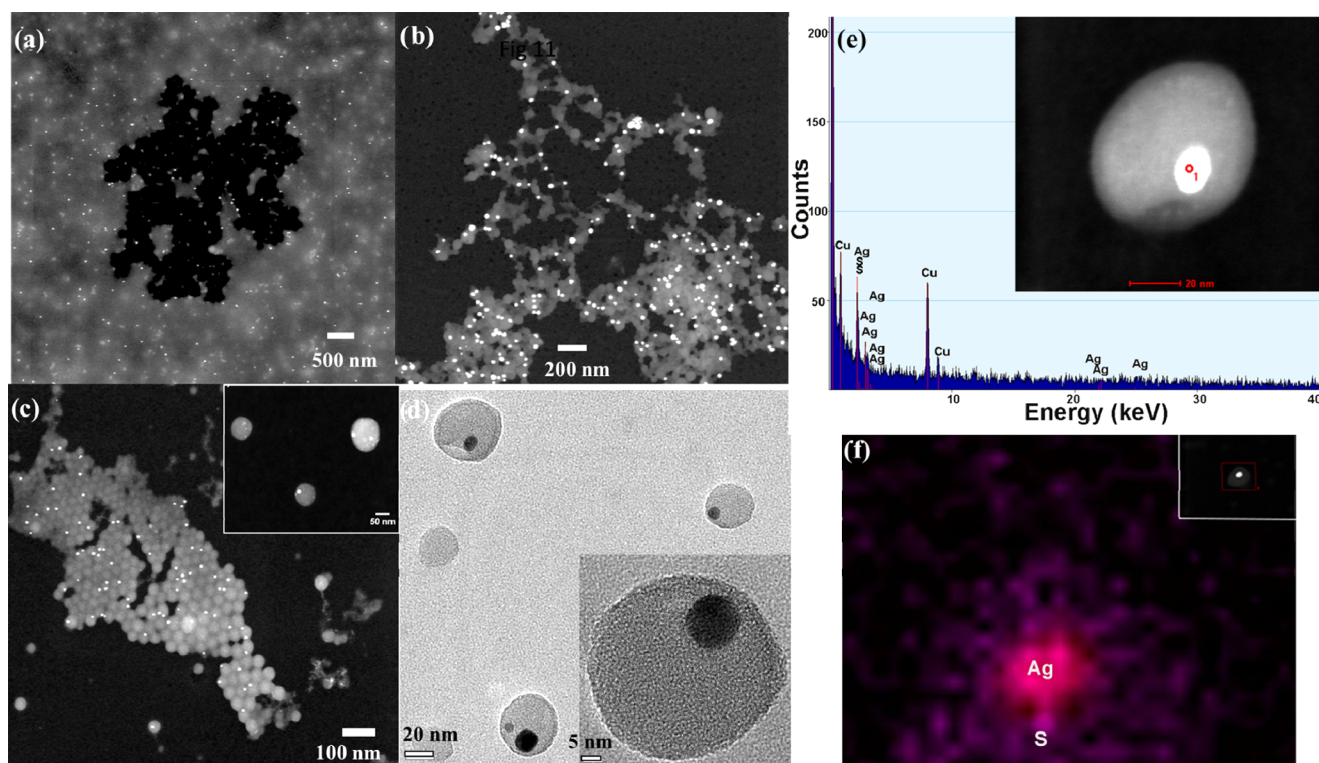


**Figure 4.** TEM images for the oligomer to silver ratio as (a) 1:4, (b) 1:2, (c) 2:1, and (d) 4:1 and single oligomer–silver hybrid nanoparticle as inset, (e) the EDX spectrum of a hybrid nanoparticle (one of the hybrid nanoparticles shown in micrograph (d)) and focus given as inset, (f) elemental mapping is also performed for Ag and S and drift-corrected image given as inset. (TEM micrograph of a single oligomer nanoparticle given as inset in (d) for the 4:1 (oligomer/Ag) sample is measured as 47 nm with GATAN digital micrograph software, and the diameter of the silver nanoparticle is found as 13 nm).

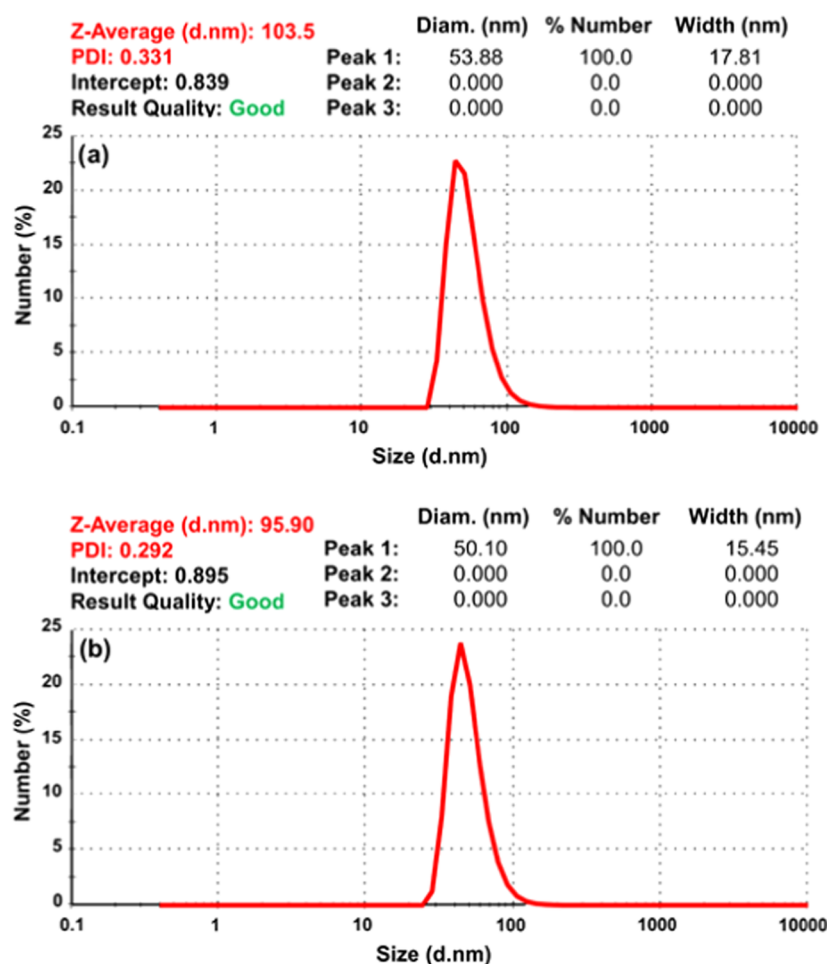


**Figure 5.** DLS histograms of (a) COL-NPs and (b) hybrid COL-Ag NPs (COL/AgNO<sub>3</sub>, 4:1).

light scattering (DLS) and TEM as around  $70 \pm 10$  nm (Figure 2a).

To prepare hybrid COL-NPs with silver NPs, aqueous silver nitrate solution was added at varying ratios to the preprepared COL-NPs aqueous dispersion. The mixture was sonicated for a few minutes and kept in an airtight container for at least 24 h at room temperature to allow for AgNP formation before opening the flask. The reaction of AgNP formation was monitored by UV–vis spectroscopy. Figure 1 shows the UV–vis absorption and photoluminescence (PL) spectra of COL-NP only and hybrid nanoparticles (COL-NP@AgNP) with increasing concentration of Ag. At low concentration of AgNO<sub>3</sub>, changes in their UV–vis absorption bands are not significant but from the ratio of 1:2 for COL-NP to AgNO<sub>3</sub>, the plasmonic band of the AgNPs is apparent as a shoulder at around 445 nm. The plasmonic band at 445 nm gradually increases with the increasing concentration of Ag. In the PL intensity, a slight increase is observed at the low concentrations of Ag but starting from the ratio of 1:2 for COL to AgNO<sub>3</sub>, PLs of the COL-NPs are quenched significantly.

To confirm the formation of AgNPs and investigate the morphology of the hybrid structures, we recorded their transmission electron microscope (TEM) images, as given in Figure 2. As can be seen from the TEM micrograph of the sample prepared at room temperature (COL/AgNO<sub>3</sub>, 1:8), silver nanoparticles decorated the surface of the nanoparticles. Figure 2b focuses on COL-NP with 88 nm diameter decorated with 9.7 nm diameter AgNPs. There are also some debris-like

residues, which are probably Ag clusters that will coalesce to form larger AgNPs over time. Figure 2c shows the coalesced small AgNPs leading to large particles on the periphery of the COL-NPs. In the focused micrograph, COL-NP, with a diameter of 77 nm, was surrounded by AgNPs with 18 nm diameter. Over time, large aggregates and network type hybrid structures are formed (Figure 2d).

**Details of Route B.** In this route, hybrid nanoparticles were prepared by injecting the THF solution of COL into aqueous solution of AgNO<sub>3</sub>. The mixture was sonicated for 30 min and then THF was removed under reduced pressure to obtain stable hybrid COL-Ag NPs in water. COL to Ag ratios, such as 1:1, 1:2, 1:4, 2:1, 3:1, and 4:1, were used to investigate the concentration effect of silver in the hybrid nanoparticle formation. Figure 3 shows the UV–vis and fluorescent spectra of these nanoparticles prepared at different ratios. As can be seen from the UV–vis spectra, even at the lowest concentration of Ag, the plasmonic band of AgNPs appears at around 428 nm and at high concentrations its intensity increases. Although there is a decrease in the fluorescence emission intensity even at low Ag concentrations, this decrease is not as significant as in the hybrid nanoparticles prepared in route A. Especially at the low concentrations of Ag, there is about a 30% decrease in the PL intensity.

To reveal their morphologies and sizes, their TEM images were taken (Figure 4). As can be seen from the TEM micrograph of the hybrid NPs, with the COL to Ag ratio of 1:4 (Figure 4a), although AgNPs are evenly distributed, high

concentration of Ag causes the formation of aggregation and network type structures (Figure 4a,b). By decreasing the initial concentration of Ag ions, the hybrid nanoparticles become more ordered and homogenous. The results indicate that depending on the ratios of COL to Ag ions, it is possible to control the sizes of hybrid nanoparticles and to prevent aggregate formation. It seems that the ratios of COL to Ag ions of 2:1 and lower are suitable for the synthesis of well-defined hybrid nanoparticles.

Chemical composition of the hybrid nanoparticles with the COL to Ag ratio of 4:1 (Figure 4d) was further investigated with energy dispersive X-ray spectroscopy (EDX), shown in Figure 4e, with the focus point given as inset. The spectrum confirms the presence of silver as well as sulfur present in the structure of COL, and Cu signal comes from the TEM grid. Elemental mapping is further performed using drift correction, and given in Figure 4f. Ag is shown by pink and sulfur by purple.

Their sizes were also measured by dynamic light scattering (DLS) (Figure 5). In the case of the samples with high Ag concentrations, we were not able to obtain reliable results because of the aggregate formation, as this can also be seen in their TEM images. However, the diameter of the hybrid nanoparticles with the ratios of COL to Ag as 2:1 and lower were measured to be around  $50 \pm 5$  nm. The sizes of COL-NPs without Ag are also in the same range. These results are also in line with the results taken from TEM images. For example, TEM image of a single hybrid oligomer–Ag nanoparticle given as inset in Figure 4d for the 4:1 (oligomer–Ag) sample is measured as 47 nm with GATAN digital micrograph software and diameter of AgNPs is found as 13 nm.

Although we were not able to obtain a satisfactory XRD spectrum with the hybrid NPs with low concentration of silver, the crystalline nature of silver nanoparticles can be inferred from their TEM micrographs. For instance, a TEM micrograph of one of the hybrid COL–Ag NPs with low concentration of Ag composition (the ratio of 1:1) in Figure 6 (right panel)

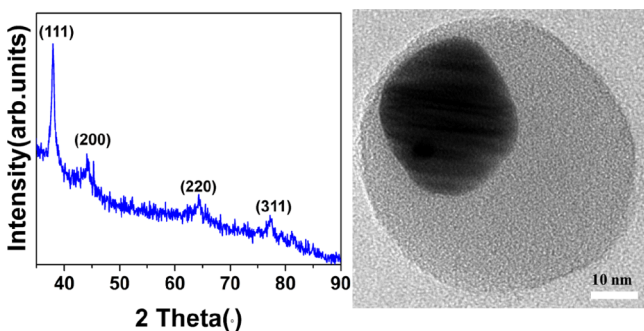


**Figure 6.** TEM micrographs of the hybrid COL–Ag NPs with the ratio of 1:1, COL to Ag (right panel); XRD pattern of the hybrid COL–Ag NPs with the ratio of 1:4, COL to Ag (left panel).

shows regularly spaced horizontal lines probably due to the interplanar spacing of the lattice fringe. However, this should be further supported by taking the selected area diffraction pattern. Figure 6 (right panel) shows a TEM micrograph of one of the hybrid COL–Ag NPs with low concentration of Ag composition (the ratio of 1:1). However, COL to Ag ratio of 1:4 allowed us to do the XRD analysis for the hybrid NPs. XRD pattern of the hybrid COL–Ag NPs is shown in Figure 6 (left panel).

To prepare the sample for XRD analysis, the solution was drop casted onto very thin glass and the zero background holder was used in Theta/2 geometry. The spectrum was recorded at  $30\text{--}90^\circ$  using 0.05 step size and 45 s of counting time. Peaks were observed at  $37.9$ ,  $44.2$ ,  $64.3$ , and  $77.5^\circ$  corresponding to planes (111), (200), (220), and (311) of the face-centered cubic (FCC)-structured silver nanocrystal, with reference number (ICDD reference code: 98-018-0878).

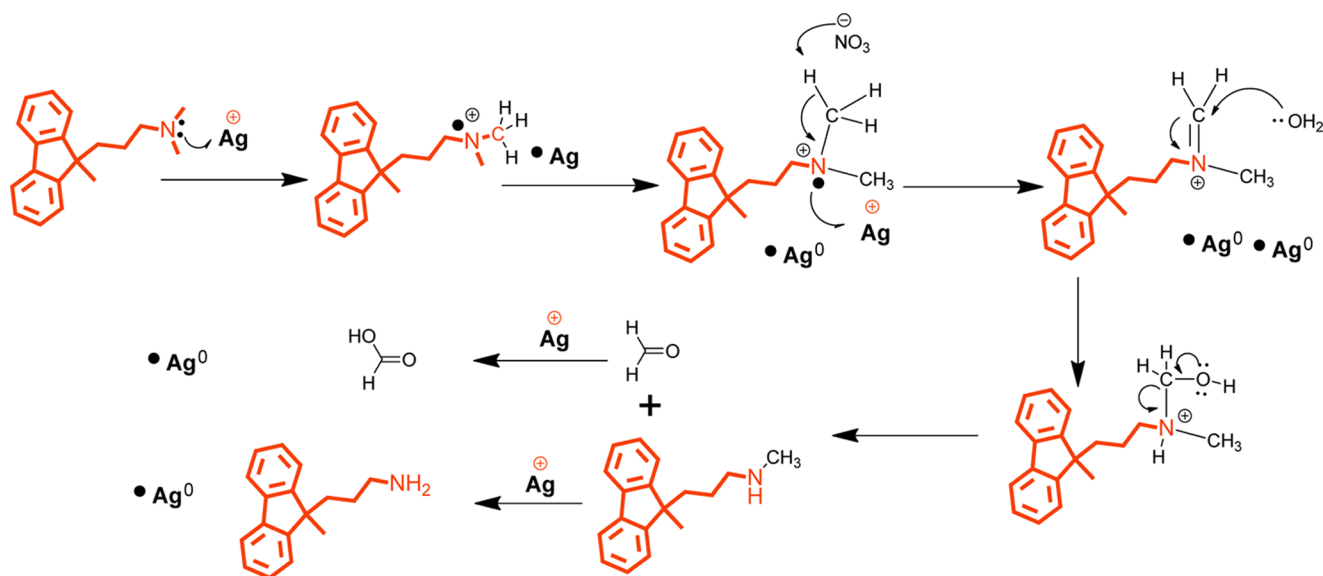
On the basis of the literature precedents,<sup>45–48</sup> we propose the following reaction mechanism (Scheme 2) for the reduction of Ag ions to Ag(0) and subsequent AgNP formation. The mechanisms are expected to be slightly different in each route due to different coordination modes of silver ions. In route A, the AgNP formation was observed to be slower than that in route B. In route A, silver ions use the available surface amine groups and may be aromatic fluorene and benzothiazole groups are less likely accessible for the coordination of Ag ions. As suggested in the reaction mechanism scheme, probably due to close proximity of silver ions with amine groups, one electron of the nitrogen of amine is transferred to  $\text{Ag}^+$ , reducing  $\text{Ag}^+$  to Ag(0), and itself becomes a radical cation by transferring a second electron of the radical cation to another silver. The subsequent abstraction of one of the protons of the methyl group by a nitrate ion will form an imine which will be further attacked by water molecules by leading a simultaneous departure of formaldehyde to leave behind secondary amine. After the formation of formaldehyde, reduction of the remaining silver ions are expected to be faster. Silver ions are reduced to metallic silver, and formaldehyde is oxidized to formic acid.

In the case of route B, first, silver ions will be captured by COL chains and then self-assembled Ag ions containing nanostructures will be formed. Confined silver ions can coordinate with sulfur residues and benzene rings of the oligomer backbone, forming  $\pi$ -ion complexes as well as coordinating with amine groups. In the confined environment, the electron transfer from amine nitrogen to Ag ion and the consequent reduction of silver ions with the above proposed reaction mechanism would be faster as the interior of the COL-NP will be providing the microenvironment for the silver ions by catalyzing oxidation of tertiary alkyl amine and reducing silver ions to metallic silver. Moreover, formaldehyde formed during this reaction will be again confined in this environment for further reaction with the available silver ions.

## CONCLUSIONS

We reported the one-pot, straightforward synthesis of hybrid conjugated oligomer with silver nanoparticles. We have tried two different methods to prepare nanostructures. In the first method, first, COL-NPs were prepared and these COL-NPs were decorated with AgNPs. COL-NPs acted here as the reductant and supporting frame for the newly formed AgNPs to be attached. There are some drawbacks in this design. AgNPs' formation is slow, and it is difficult to control the sizes of AgNPs as the small particles coalesce by forming larger nanoparticles. Moreover, PL of the COL-NPs are significantly quenched and at high silver concentration aggregates are formed. Using the second method, it is possible to control the sizes and the morphology of the hybrid nanoparticles. This method is simpler than the first method; hybrid nanoparticles are prepared in a single step by injecting COL solution into aqueous silver nitrate solution. AgNPs are formed in the interior of the COL-NPs by the reduction of silver ions. There

**Scheme 2.** Proposed Reaction Scheme for the Reduction of Silver Ions to Metallic Silver and as a Result the Formation of Silver Nanoparticles



is no need to use an extra reducing agent as COL acts as a reducing agent as well as a matrix to encapsulate the newly formed AgNPs. Moreover, with this method, by carefully adjusting the ratio of COL to Ag, we will be able to keep PL properties of COL. We have also applied the second method for the synthesis of gold nanoparticles, and our preliminary results show the success of the method in the formation of gold nanoparticles. Currently, we are working on the synthesis of other hybrid nanoparticles using this method and exploring the application of these hybrid NPs in various areas. We believe that these hybrid nanoparticles could find variety of applications including photocatalysis, plasmonic sensing, and theranostics.

## METHODS

Optical properties of oligomer nanoparticles and silver-decorated oligomer nanoparticles were characterized by a UV–vis spectrophotometer (Carry, UV–vis) and a fluorescence spectrophotometer (Carry Eclipse Fluorescent Spectrophotometer). The morphologies of oligomer and silver nanoparticle were investigated using focused ion beam scanning electron microscopy (FEI, NanoSEM) and transmission electron microscopy (FEI Technai G2 F30). Determination of the size distribution and average diameter of nanoparticles with respect to their hydrodynamic sizes were carried out via dynamic light scattering (DLS) measurements (Malvern Nano-ZS Zetasizer). Chemical and elemental analysis of nanoparticles were determined using X-ray photoelectron spectroscopy (XPS) (Thermo Fisher Scientific). Measurements were performed with a spot size of  $\sim 400 \mu\text{m}$ , 30 eV pass energy, and 0.1 eV step size. The powder X-ray diffraction system (X'pert pro MPD (PANalytical)) to study the XRD patterns of the hybrid materials.

All chemicals and solvents were purchased from Sigma Aldrich Chemical Co. (Germany), including silver nitrate salt. Detailed synthesis and characterization of the oligomer were reported in our previous publications.<sup>30,33</sup>

**Synthesis of Nanoparticles. Route A:** 1 mL of the THF solution of COL (1 mg/1 mL) was injected into 4 mL of deionized water in an ultrasonic bath for 30 min, and then THF

was removed under reduced pressure. To prepare hybrid nanoparticles with COL to Ag ratios of 4:1, 2:1, 1:1, 1:2, 1:4, and 1:8, aqueous AgNO<sub>3</sub> solutions in predetermined concentrations were added to preprepared aqueous dispersion of COL-NPs. The mixture was sonicated for 5 min.

**Route B:** Hybrid COL-Ag NPs were prepared, with the COL to AgNO<sub>3</sub> ratios as 4:1, 3:1, 2:1, 1:1, 1:2, and 1:4.

*In a Typical Hybrid NP Synthesis (COL to AgNO<sub>3</sub>, 1:1).* COL (4.0 mg, 4.7  $\mu\text{mol}$ ) was dissolved in 10 mL of THF. AgNO<sub>3</sub> (5.0 mg, 29.4  $\mu\text{mol}$ ) was dissolved in 10 mL of distilled water. AgNO<sub>3</sub> (aq) solution (160  $\mu\text{L}$ ) was placed into a flask and the total volume was made up to 5 mL with distilled water. During the sonication, 1 mL of the THF solution of COL was added into this flask and the sonication continued further for 30 min. THF was removed under reduced pressure to leave behind the dispersion of hybrid nanoparticles.

## AUTHOR INFORMATION

### Corresponding Author

\*E-mail: dtuncel@fen.bilkent.edu.tr.

### ORCID

Dönüs Tuncel: 0000-0001-7762-9200

### Notes

The authors declare no competing financial interest.

## ACKNOWLEDGMENTS

D.T. acknowledges TUBITAK-TBAG 114Z195.

## REFERENCES

- (1) Huynh, W. U.; Dittmer, J. J.; Alivisatos, A. P. Hybrid nanorod-polymer solar cells. *Science* **2002**, *295*, 2425–2427.
- (2) Sanchez, C.; Julian, B.; Belleville, P.; Popall, M. Applications of hybrid organic–inorganic nanocomposites. *J. Mater. Chem.* **2005**, *15*, 3559–3592.
- (3) Atwater, H. A.; Polman, A. Plasmonics for improved photovoltaic devices. *Nat. Mater.* **2010**, *9*, 205–213.
- (4) Zhou, N.; Lopez-Puente, V.; Wang, Q.; Polavarapu, L.; Pastoriza-Santos, I.; Xu, Q.-H. Plasmon-enhanced light harvesting: applications in enhanced photocatalysis, photodynamic therapy and photovoltaics. *RSC Adv.* **2015**, *5*, 29076–29097.

- (5) Noginov, M. A.; Zhu, G.; Belgrave, A. M.; Bakker, R.; Shalaev, V. M.; Narimanov, E. E.; Stout, S.; Herz, E.; Suteewong, T.; Wiesner, U. Demonstration of a spaser-based nanolaser. *Nature* **2009**, *460*, 1110–1112.
- (6) Matsuhisa, N.; Inoue, D.; Zalar, P.; Jin, H.; Matsuba, Y.; Itoh, A.; Yokota, T.; Hashizume, D.; Someya, T. Printable elastic conductors by in situ formation of silver nanoparticles from silver flakes. *Nat. Mater.* **2017**, *16*, 834.
- (7) Hussain, I.; Brust, M.; Papworth, A. J.; Cooper, A. I. Preparation of Acrylate-Stabilized Gold and Silver Hydrosols and Gold-Polymer Composite Films. *Langmuir* **2003**, *19*, 4831–4835.
- (8) Bao, Y.; Shen, G.; Liu, H.; Li, Y. Fabrication of gold nanoparticles through autoreduction of chloroaurate ions by thermo- and pH-responsive amino acid-based star-shaped copolymers. *Polymer* **2013**, *54*, 652–660.
- (9) Oishi, M.; Hayashi, H.; Uno, T.; Ishii, T.; Iijima, M.; Nagasaki, Y. One-Pot Synthesis of pH-Responsive PEGylated Nanogels Containing Gold Nanoparticles by Autoreduction of Chloroaurate Ions within Nanoreactors. *Macromol. Chem. Phys.* **2007**, *208*, 1176–1182.
- (10) Ishii, T.; Otsuka, H.; Kataoka, K.; Nagasaki, Y. Preparation of Functionally PEGylated Gold Nanoparticles with Narrow Distribution through Autoreduction of Auric Cation by  $\alpha$ -Biotinyl-PEG-block-[poly(2-(N,N-dimethylamino)ethyl methacrylate)]. *Langmuir* **2004**, *20*, 561–564.
- (11) Ray, D.; Aswal, V. K.; Kohlbrecher, J. Synthesis and Characterization of High Concentration Block Copolymer-Mediated Gold Nanoparticles. *Langmuir* **2011**, *27*, 4048–4056.
- (12) Leiva, A.; Saldías, C.; Quezada, C.; Toro-Labbé, A.; Espinoza-Beltrán, F. J.; Urzúa, M.; Gargallo, L.; Radic, D. Gold-copolymer nanoparticles: Poly( $\epsilon$ -caprolactone)/poly(N-vinyl-2-pyrrolidone) Biodegradable triblock copolymer as stabilizer and reductant. *Eur. Polym. J.* **2009**, *45*, 3035–3042.
- (13) Sawada, H.; Takahashi, K. Facile preparation of gold nanoparticles through autoreduction of gold ions in the presence of fluoroalkyl end-capped cooligomeric aggregates: LCST-triggered sol-gel switching behavior of novel thermoresponsive fluoroalkyl end-capped cooligomeric nanocomposite-encapsulated gold nanoparticles. *J. Colloid Interface Sci.* **2010**, *351*, 166–170.
- (14) Meristoudi, A.; Pispas, S. Polymer mediated formation of corona-embedded gold nanoparticles in block polyelectrolyte micelles. *Polymer* **2009**, *50*, 2743–2751.
- (15) Sakai, T.; Alexandridis, P. Mechanism of Gold Metal Ion Reduction, Nanoparticle Growth and Size Control in Aqueous Amphiphilic Block Copolymer Solutions at Ambient Conditions. *J. Phys. Chem. B* **2005**, *109*, 7766–7777.
- (16) Kohut, A.; Voronov, A.; Samaryk, V.; Peukert, W. Amphiphilic Invertible Polyesters as Reducing and Stabilizing Agents in the Formation of Metal Nanoparticles. *Macromol. Rapid Commun.* **2007**, *28*, 1410–1414.
- (17) Kavitha, M.; Parida, M. R.; Prasad, E.; Vijayan, C.; Deshmukh, P. C. Generation of Ag Nanoparticles by PAMAM Dendrimers and their Size Dependence on the Aggregation Behavior of Dendrimers. *Macromol. Chem. Phys.* **2009**, *210*, 1310–1318.
- (18) Strozyk, M. S.; de Aberasturi, D. J.; Gregory, J. V.; Brust, M.; Lahann, J.; Liz-Marzán, L. M. Spatial Analysis of Metal-PLGA Hybrid Microstructures Using 3D SERS Imaging. *Adv. Funct. Mater.* **2017**, *346*, No. 1701626.
- (19) Zhang, H.; Li, Y.-H.; Chen, Y.; Wang, M.-M.; Wang, X.-S.; Yin, X.-B. Fluorescence and Magnetic Resonance Dual-Modality Imaging-Guided Photothermal and Photodynamic Dual-Therapy with Magnetic Porphyrin-Metal Organic Framework Nanocomposites. *Sci. Rep.* **2017**, *7*, No. 44153.
- (20) Li, W.; Zhang, H.; Guo, X.; Wang, Z.; Kong, F.; Luo, L.; Li, Q.; Zhu, C.; Yang, J.; Lou, Y.; Du, Y.; You, J. Gold Nanospheres-Stabilized Indocyanine Green as a Synchronous Photodynamic-Photothermal Therapy Platform That Inhibits Tumor Growth and Metastasis. *ACS Appl. Mater. Interfaces* **2017**, *9*, 3354–3367.
- (21) Tuncel, D.; Demir, H. V. Conjugated Polymer Nanoparticles. *Nanoscale* **2010**, *2*, 484.
- (22) Feng, L.; Zhu, C.; Yuan, H.; Liu, L.; Lv, F.; Wang, S. Conjugated polymer nanoparticles: preparation, properties, functionalization and biological applications. *Chem. Soc. Rev.* **2013**, *42*, 6620–6633.
- (23) Jiang, Y.; McNeill, J. Light-Harvesting and Amplified Energy Transfer in Conjugated Polymer Nanoparticles. *Chem. Rev.* **2017**, *117*, 838–859.
- (24) Keita, H.; Guzelurk, B.; Pennakalathil, J.; Erdem, T.; Demir, H. V.; Tuncel, D. Construction of multi-layered white emitting organic nanoparticles by clicking polymers. *J. Mater. Chem. C* **2015**, *3*, 10277–10284.
- (25) Ozel, I. O.; Ozel, T.; Demir, H. V.; Tuncel, D. Non-radiative resonance energy transfer in bi-polymer nanoparticles of fluorescent conjugated polymers. *Opt. Express* **2010**, *18*, 670–684.
- (26) Baykal, B.; Ibrahimova, V.; Er, G.; Bengu, E.; Tuncel, D. Dispersion of multi-walled carbon nanotubes in an aqueous medium by water-dispersible conjugated polymer nanoparticles. *Chem. Commun.* **2010**, *46*, 6762–6764.
- (27) Ibrahimova, V.; Kocak, M. E.; Onal, A. M.; Tuncel, D. Optical and Electronic Properties of Fluorene-Based Copolymers and Their Sensory Applications. *J. Polym. Sci., Part A: Polym. Chem.* **2013**, *51*, 815–823.
- (28) Erdem, T.; Ibrahimova, V.; Jeon, D. W.; Lee, I. H.; Tuncel, D.; Demir, H. V. Morphology-Dependent Energy Transfer of Polyfluorene Nanoparticles Decorating InGaN/GaN Quantum-Well Nanopillars. *J. Phys. Chem. C* **2013**, *117*, 18613–18619.
- (29) Ibrahimova, V.; Ekiz, S.; Gezici, O.; Tuncel, D. Facile synthesis of cross-linked patchy fluorescent conjugated polymer nanoparticles by click reactions. *Polym. Chem.* **2011**, *2*, 2818–2824.
- (30) Pennakalathil, J.; Jahja, E.; Ozdemir, E. S.; Konu, O.; Tuncel, D. Red Emitting, Cucurbituril-Capped, pH-Responsive Conjugated Oligomer-Based Nanoparticles for Drug Delivery and Cellular Imaging. *Biomacromolecules* **2014**, *15*, 3366–3374.
- (31) Park, E.-J.; Erdem, T.; Ibrahimova, V.; Nizamoglu, S.; Demir, H. V.; Tuncel, D. White-Emitting Conjugated Polymer Nanoparticles with Cross-Linked Shell for Mechanical Stability and Controllable Photometric Properties in Color-Conversion LED Applications. *ACS Nano* **2011**, *5*, 2483–2492.
- (32) Huyal, I. O.; Ozel, T.; Tuncel, D.; Demir, H. V. Quantum Efficiency Enhancement in Film by Making Nanoparticles of Polyfluorene. *Opt. Express* **2008**, *16*, 13391–13397.
- (33) Soran-Erdem, Z.; Erdem, T.; Gungor, K.; Pennakalathil, J.; Tuncel, D.; Demir, H. V. High-Stability, High-Efficiency Organic Monoliths Made of Oligomer Nanoparticles Wrapped in Organic Matrix. *ACS Nano* **2016**, *10*, 5333–5339.
- (34) Sun, W.; Hayden, S.; Jin, Y.; Rong, Y.; Yu, J.; Ye, F.; Chan, Y.-H.; Zeigler, M.; Wu, C.; Chiu, D. T. A versatile method for generating semiconducting polymer dot nanocomposites. *Nanoscale* **2012**, *4*, 7246–7249.
- (35) Park, D. H.; Kim, M. S.; Joo, J. Hybrid nanostructures using p-conjugated polymers and nanoscale metals: synthesis, characteristics, and optoelectronic applications. *Chem. Soc. Rev.* **2010**, *39*, 2439–2452.
- (36) Wang, X.; He, F.; Zhu, X.; Tang, F.; Li, L. Hybrid silver nanoparticle/conjugated polyelectrolyte nanocomposites exhibiting controllable metal-enhanced fluorescence. *Sci. Rep.* **2014**, *4*, No. 4406.
- (37) Kim, M. S.; Park, D. H.; Cho, E. H.; Kim, K. H.; Park, Q.-H.; Song, H.; Kim, D.-C.; Kim, J.; Joo, J. Complex Nanoparticle of Light-Emitting MEH-PPV with Au: Enhanced Luminescence. *ACS Nano* **2009**, *3*, 1329.
- (38) Bhattacharyya, S.; Sen, T.; Patra, A. Host-Guest Energy Transfer: Semiconducting Polymer Nanoparticles and Au Nanoparticles. *J. Phys. Chem. C* **2010**, *114*, 11787–11795.
- (39) Mir, S. H.; Ochiai, B. One-Pot Fabrication of Hollow Polymer@Ag Nanospheres for Printable Translucent Conductive Coatings. *Adv. Mater. Interfaces* **2017**, *4*, No. 1601198.
- (40) Yang, H.; Duan, C.; Wu, Y.; Lv, Y.; Liu, H.; Lv, Y.; Xiao, D.; Huang, F.; Fu, H.; Tian, Z. Conjugated Polymer Nanoparticles with Ag<sup>+</sup>-Sensitive Fluorescence Emission: A New Insight into the Cooperative Recognition Mechanism. *Part. Part. Syst. Charact.* **2013**, *30*, 972–980.

- (41) Liu, X.; He, X.; Jiu, T.; Yuan, M.; Xu, J.; Lv, J.; Liu, H.; Li, Y. Controlled Aggregation of Functionalized Gold Nanoparticles with a Novel Conjugated Oligomer. *Chem. Phys. Chem.* **2007**, *8*, 906–912.
- (42) Jana, B.; Bhattacharyya, S.; Patra, A. Conjugated polymer P3HT–Au hybrid nanostructures for enhancing photocatalytic activity. *Phys. Chem. Chem. Phys.* **2015**, *17*, 15392–15399.
- (43) Cao, H.-L.; Huang, H.-B.; Chen, Z.; Karadeniz, B.; Lü, J.; Cao, R. Ultrafine Silver Nanoparticles Supported on a Conjugated Microporous Polymer as High-Performance Nanocatalysts for Nitrophenol Reduction. *ACS Appl. Mater. Interfaces* **2017**, *9*, 5231–5236.
- (44) Rybak, B. M.; Ornatska, M.; Bergman, K. N.; Genson, K. L.; Tsukruk, V. V. Formation of Silver Nanoparticles at the Air–Water Interface Mediated by a Monolayer of Functionalized Hyperbranched Molecules. *Langmuir* **2006**, *22*, 1027–1037.
- (45) Kanoufi, F.; Zu, Y.; Bard, A. J. Homogeneous Oxidation of Trialkylamines by Metal Complexes and Its Impact on Electro-generated Chemiluminescence in the Trialkylamine/Ru(bpy)<sub>3</sub><sup>2+</sup> System. *J. Phys. Chem. B* **2001**, *105*, 210–216.
- (46) Newman, J. D. S.; Blanchard, G. J. Formation of Gold Nanoparticles Using Amine Reducing Agents. *Langmuir* **2006**, *22*, 5882–5887.
- (47) Kuo, P.-L.; Chen, C. C. Generation of Gold Thread from Au(III) and Triethylamine. *Langmuir* **2006**, *22*, 7902–7906.
- (48) Silver Nanoparticles Capped by Oleylamine: Formation, Growth, and Self-Organization, Chen, M.; Feng, Y.-G.; Wang, X.; Li, T.-C.; Zhang, J.-Y.; Qian, D.-J. *Langmuir* **2007**, *23*, 5296–5304.